

OMAE2017-62447

## HYDRODYNAMIC COEFFICIENTS FOR SUCTION ANCHORS DURING INSTALLATION OPERATIONS

Frøydis Solaas  
SINTEF Ocean <sup>1</sup>  
Trondheim, Norway

Peter Christian Sandvik  
PC Sandvik Marine  
Trondheim, Norway

### ABSTRACT

Increasing demands on economy in the offshore industry and extension to North Atlantic all-year operations bring along a requirement for more accurate numerical simulations of marine installation operations. These simulations will assess the necessary vessel and crane capacity and determine the limiting sea state for the installation. An essential input to such analysis is hydrodynamic coefficients for the structures to be installed. Together with the vessel capacity, the limiting sea-state will, in many cases be dependent on the coefficients used in the simulations. A realistic estimate of the coefficients for the structure in question will therefore have directly influence on the cost of the operation. Coefficients for hydrodynamic added mass and damping for simple geometries are given in standard textbooks and in the "Recommended practice for modelling and analysis of marine operations", DNVGL-RP-H103. For more complex structures and structure parts on the other hand, there is a lack of published data. MARINTEK and NTNU have through the last decades performed model testing of different structural details as well as complete subsea structures. During the research program MOVE, started in 2015 by NTNU, MARINTEK and SINTEF, a considerable amount of model test data is collected and compared to obtain general trends and connections suitable for engineering estimates of coefficients to be used in numerical simulations. Suction anchors are widely used for permanent mooring of floating production and storage vessels, and also for foundation of subsea structures. In several cases use of suction anchors have replaced piling for foundation of offshore wind turbines and jacket platforms. The anchors can be exposed to high hydrodynamic forces during the installation. This paper presents hydrodynamic coefficients in heave for suction anchors with different degree of perforation of the top

plate and different height/diameter relations. The results range from anchors with no perforation to around 18% perforation.

### INTRODUCTION

A typical suction anchor is a steel cylinder with closed top. One or more hatches are arranged in the top in order to evacuate air during water entry and to provide ventilation during lowering, landing and soil penetration. After completed self penetration the top hatch covers are closed and suction can be applied through valves, for final penetration and levelling. In most cases the vertical side walls are without holes. However, in some cases the lower part of the walls may be perforated in order to reduce the risk for soil fracture during landing and the initial part of the soil penetration. The diameter to height ratio can vary considerably, depending on usage and soil conditions.



FIGURE 1. EXAMPLE OF SUBSEA STRUCTURE WITH SUCTION ANCHORS. MODEL OF THE GJØA TEMPLATE.

<sup>1</sup> Earlier MARINTEK, SINTEF Ocean from 1<sup>st</sup> January 2017 through a merger internally in the SINTEF Group

Rough estimations for hydrodynamic coefficients for structures with vertical sides and different degree of perforation are given in DNVGL-RP-H103 [1]. These estimations will generally overestimate the added mass for perforated suction anchors, which is the intension in the recommendations. But the amplitude dependence of the added mass is not taken into account and for small perforations and large oscillations the recommendations will underestimate the added mass compared with the results from model tests.

In this paper data for suction anchors with closed top and with one or more open hatches in the top plate are presented. The diameter to height ratio varies between 0.42 and 1.25.

In most cases a suction anchor has the center axis vertical throughout the whole installation operation. Therefore, this paper describes hydrodynamic added mass and damping for vertical motion (heave) only.

### NOMENCLATURE

- $A_{33}$  Added mass in vertical direction (kg)
- $A_0$  Added mass in vertical direction, for suction anchor without or with closed ventilation hatches (kg)
- $B_{33}$  Linear damping in vertical direction (Ns/m)
- $B_1$  Linear damping constant (Ns/m)
- $B_2$  Quadratic damping constant (Ns<sup>2</sup>/m<sup>2</sup>)
- $C_d$  Quadratic drag coefficient (-)
- D/R Diameter/radius of suction anchor (m)
- H Height of suction anchor (m)
- p Porosity, ventilation area ratio,  $p = S_h/S$  (-)
- S Top area of suction anchor (m<sup>2</sup>)
- $S_h$  Area of open ventilation hatch(es) (m<sup>2</sup>)
- KC<sub>por</sub> Porous KC number (-)
- T Oscillation period (s)
- v Relative vertical velocity between the anchor and wave (m/s)
- Z Oscillation amplitude (m)
- $\rho$  Seawater density (kg/m<sup>3</sup>)
- $\mu$  Pressure loss parameter

### TEST METHOD

The test method used to estimate the hydrodynamic coefficients for the suction anchors presented are the motion decay method.

The test object, which is suspended in a spring with known stiffness, is released from an offset position, to undergo a free oscillation decay. The peak value at each half cycle in the motion time series is identified. The (linear) damping for each oscillation cycle is found from the motion decay from one peak to the next. The total oscillating mass is derived from the undamped natural frequency of the system, which is determined from the time between subsequent peaks, adjusted for damping. The hydrodynamic mass is found by extracting the oscillating mass of object and suspension system, which is obtained by similar oscillations in air. The motion frequency is varied by changing the spring stiffness.

A typical example of the time series for a motion decay of a suction anchor is shown in FIGURE 2 and the test setup in FIGURE 3.

The motion decay method will be inaccurate for set-ups with large relative damping, due to few obtainable oscillation cycles. However, it is well suited for systems with low damping. The curves for estimated added mass and damping often show some scatter, caused by inaccurate read-out of peak values and cycle periods. The first decay cycles should be analyzed with care because the flow has a transient nature.

The method has a weakness in cases where the added mass is much smaller than the structure mass. The practical implications of this is, however small, because the total dynamic mass is established with acceptable accuracy.

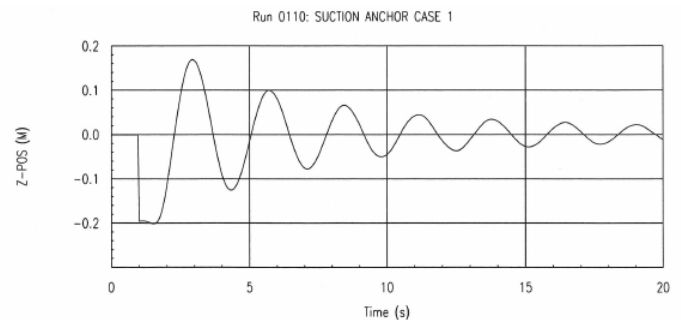


FIGURE 2. EXAMPLE OF THE TIME SERIES OF MOTION DECAY FOR A SUCTION ANCHOR.

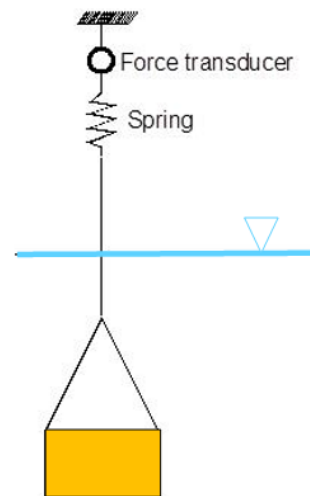


FIGURE 3. TYPICAL TEST SETUP FOR MOTION DECAY TESTS.

### TESTED SUCTION ANCHORS

During the last 20 years various types of suction anchors have been tested by MARINTEK and by MSc candidates at NTNU. Diameter to height ratio as well as number, geometry and size of holes in the top plate were varied within practical limits. TABLE 1 and FIGURE 4 gives an overview of tested items. The results are scaled to a diameter D=5 m for all anchors.

Most of the test results are unpublished, being results from commercial projects. Hydrodynamic coefficients for anchor type D with rectangular hatches is given in Sandvik et al. 2016 [2].

Some of the test results for the anchor with  $D/H = 1.25$  (O3 and B) is a part of the work for a MSc. thesis by Karlsten in 1993 [3], which also contains data for anchors with perforation of the sidewalls.

**TABLE 1 SUCTION ANCHORS TESTED**

Ident.	D/H	# holes	Geometry of holes	Perforation p (%)
O1	0.417	0	-	0
O2	0.56	0	-	0
O3	1.25	0	-	0
A	0.50	1	Circ.	1, 3, 11
B	1.25	1	Circ.	2.56
C	0.56	1,2,4	Circ.	1, 4, 6
D	0.417	1,2,3,4	Rect.	4.6, 9.2, 13.8, 18.4

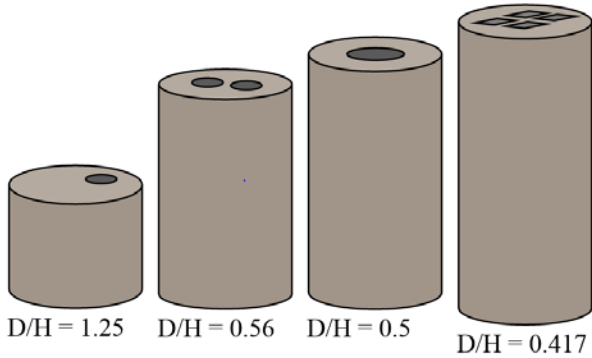


**FIGURE 4. SUCTION ANCHORS WITH DIFFERENT DIAMETER TO HEIGHT RELATION AND DIFFERENT PERFORATION OF THE TOP PLATE.**

### SUCTION ANCHORS WITHOUT PERFORATION

Added mass and damping for simple geometries without ventilation openings are found in several textbooks, and also in DNVGL-RP-H103 [1]. For  $D/H$  ratios larger than 2, the added mass of a suction anchor without holes can be found as:

$$A_0 = \rho \cdot \pi \cdot R^2 \left( H + \frac{4}{3}R \right) \quad (1)$$

where the first part corresponds to the displacement of a cylinder with radius  $R$  and height  $H$  and the second part a circular sphere with radius  $R$ .

The quadratic damping constant is defined as:

$$B_2 = \frac{1}{2} \rho \cdot C_d \cdot \pi R^2 \quad (2)$$

Notice that both  $A_0$  and  $C_d$  are assumed to be independent of oscillation frequency and amplitude.

Three models of suction anchors without perforation (O1, O2 and O3 in TABLE 1) have been tested using the motion decay method. The derived added mass in vertical direction divided by  $A_0$  is shown in FIGURE 5. The curves gather closely around the expected value for unperforated anchors, supporting the assumption that the added mass for unperforated anchors can be regarded to be independent of oscillation period and amplitude. The graphs show some scatter, which is expected for this test method.

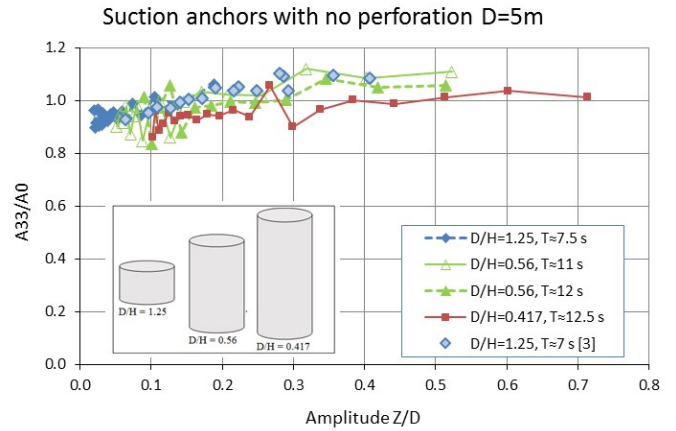


**FIGURE 5. ADDED MASS OF UNPERFORATED SUCTION ANCHORS FROM DECAY TESTS.**

The linear, vertical damping derived from the tests is shown in FIGURE 6, where the damping is plotted as function of an equivalent velocity:  $16/3 \cdot Z/T$ . Here  $Z$  is the amplitude of oscillation and  $T$  is the period.

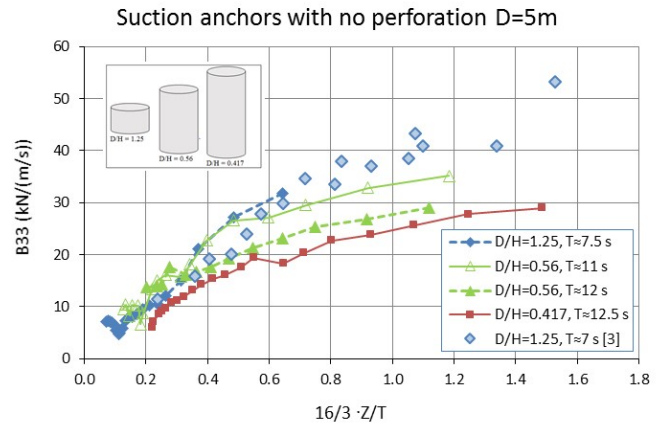


**FIGURE 6. LINEAR DAMPING OF UNPERFORATED SUCTION ANCHORS, FROM DECAY TESTS.**

When plotted in this way, the quadratic damping constant  $B_2$  is found as the gradient of a straight line fitted to the measured values. A linear damping constant  $B_1$  is found at the intersection between the same line and the ordinate axis ( $Z=0$ ). The graph shows that the damping varies with amplitude and period.

Straight lines fitted to the curves expressing the largest and operationally relevant amplitudes, gives the estimated values for

linear damping  $B_1$ , quadratic damping  $B_2$  and  $C_d$  that are summarized in TABLE 2.

**TABLE 2. ESTIMATED DAMPING PARAMETERS, UNPERFORATED SUCTION ANCHORS.**

D/H	0.42	0.56	1.25
$B_1$ (kNs/m)	15	15-20	15
$B_2$ (kNs <sup>2</sup> /m <sup>2</sup> )	10	15	25
$C_d$	1.0	1.5	2.5

The total damping force on the anchor is then given by:

$$F_D = B_1 \cdot v + B_2 \cdot v |v| \quad (3)$$

where  $v$  is the relative vertical velocity between the anchor and the waves. The given drag coefficient  $C_d$  is calculated from (2) and contains only the contribution from the quadratic term  $B_2$ .

DNVGL-RP-H103 [1] suggests the following drag coefficients in vertical direction:

$$\begin{matrix} D/H = & 0.42 & 0.56 & 1.25 \\ C_d = & 0.85 & 0.86 & 0.95 \end{matrix}$$

The estimated drag coefficients are higher than the values suggested by DNVGL, which are most probably valid for stationary flow. Estimates based on smaller amplitudes (cf. FIGURE 6) would show even larger difference to the DNVGL values.

## SUCTION ANCHORS WITH VENTILATED TOP PLATE

### Anchor with D/H = 0.5

Added mass and damping for anchor type A with  $D/H = 0.5$  and one circular hole of varying diameter is shown in FIGURE 7 and FIGURE 8, respectively. Tests are performed for different periods of oscillation. It is seen that the added mass for this anchor is independent of the period of oscillation, but dependent on the amplitude.

The damping values are dependent on both amplitude and period of oscillation. The periods of oscillation during the decays are shown in FIGURE 9. When the obtained damping is multiplied with the period of oscillation, as shown in FIGURE 10, the curves for each degree of perforation coincide.

For perforation 11% there is a distinct difference in the damping for small and large amplitudes of oscillations. For equivalent velocities  $16/3 \cdot Z/T$  less than around 0.2, the damping is mainly quadratic and for larger amplitudes the damping mainly linear. For perforation 1 and 3% the damping is less and will have both linear and quadratic terms, with larger linear term for 3% than for 1% opening.

When the damping multiplied with the period of oscillation, as shown in FIGURE 10 is divided by the added mass, a relation between the added mass and damping is obtained. It is seen from FIGURE 11 that the damping is getting larger relative to the added mass for increasing degree of perforation.

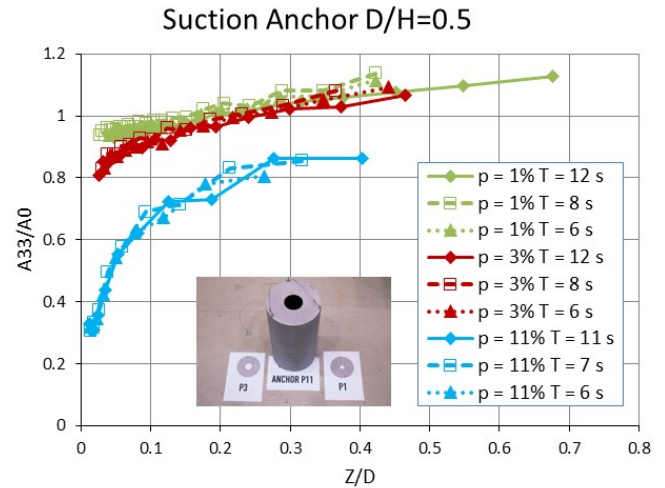


**FIGURE 7. ADDED MASS FOR SUCTION ANCHORS WITH ONE VENTILATION HOLE OF DIFFERENT SIZE, FROM DECAY TESTS. ANCHOR TYPE A.**

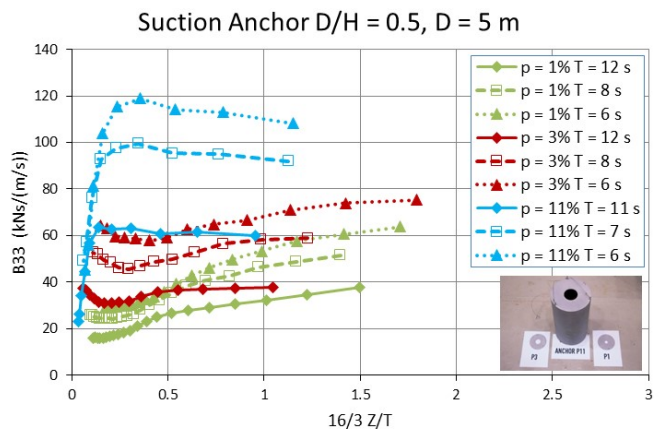


**FIGURE 8. DAMPING FOR SUCTION ANCHORS WITH ONE VENTILATION HOLE OF DIFFERENT SIZE, FROM DECAY TESTS. ANCHOR TYPE A.**

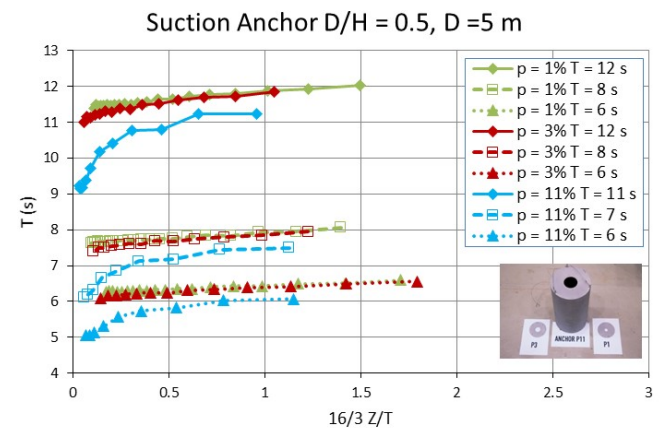


**FIGURE 9. PERIOD OF OSCILLATION DURING DECAY TESTS OF SUCTION ANCHORS WITH ONE VENTILATION HOLE OF DIFFERENT SIZE. ANCHOR TYPE A.**

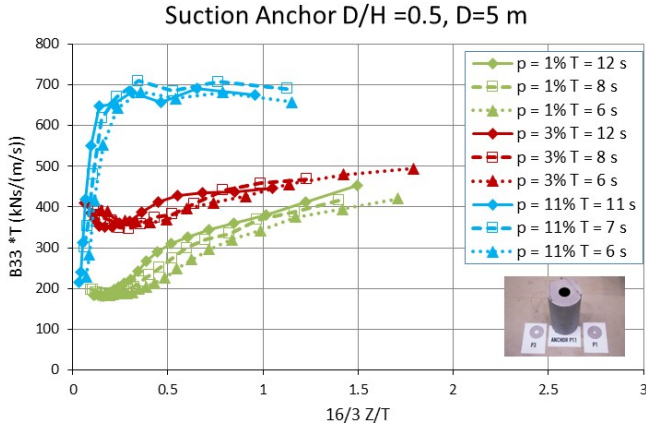


**FIGURE 10. DAMPING TIMES PERIOD OF OSCILLATION FOR SUCTION ANCHORS WITH ONE VENTILATION HOLE OF DIFFERENT SIZE. ANCHOR TYPE A.**

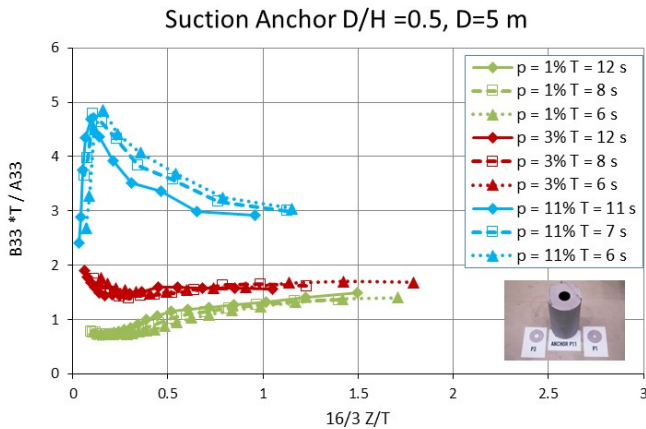


**FIGURE 11. DAMPING TIMES PERIOD OF OSCILLATION DIVIDED BY ADDED MASS FOR SUCTION ANCHORS WITH ONE VENTILATION HOLE OF DIFFERENT SIZE. ANCHOR TYPE A.**

**Anchor with D/H = 1.25**

Added mass and damping for anchor type B with D/H = 1.25 and one circular hole in the top plate is shown in FIGURE 12 and FIGURE 13, respectively.

It is seen that the added mass for large amplitudes of oscillation is close to the values without top hole and decreases for decreasing amplitude of oscillation. Linear and quadratic damping  $B_1 = 19 \text{ kNs/m}$  and  $B_2 = 30 \text{ kNs}^2/\text{m}^2$  is obtained by fitting a straight line to the curve in FIGURE 13.

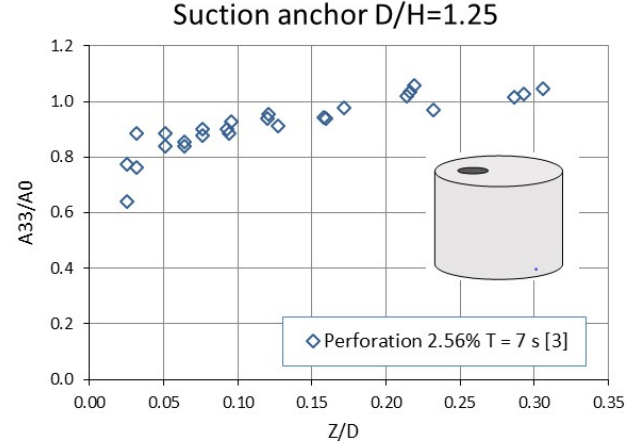


**FIGURE 12. ADDED MASS FOR ANCHOR WITH ONE TOP HOLE. MODEL TEST RESULTS FROM [3]. ANCHOR TYPE B.**

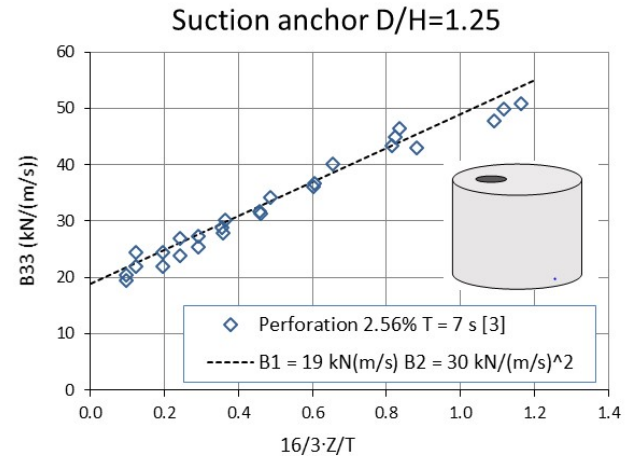


**FIGURE 13. DAMPING FOR ANCHOR WITH ONE TOP HOLE. MODEL TEST RESULTS FROM [3]. ANCHOR TYPE B.**

**Anchor with D/H = 0.56**

Added mass and damping for anchor type C with D/H = 0.56 and one or more circular holes in the top plate is shown in FIGURE 14 and FIGURE 15, respectively.

It is seen that the added mass coefficients assemble around 1.0 for the larger amplitudes and decreases for smaller amplitudes. Increasing ventilation generally decrease the added mass. Regarding the damping, it is mainly linear for the largest perforation (6%) and for the largest amplitudes for 4% perforation with 1 hole. The linear term decreases when the perforation is getting smaller and the quadratic contribution increases.

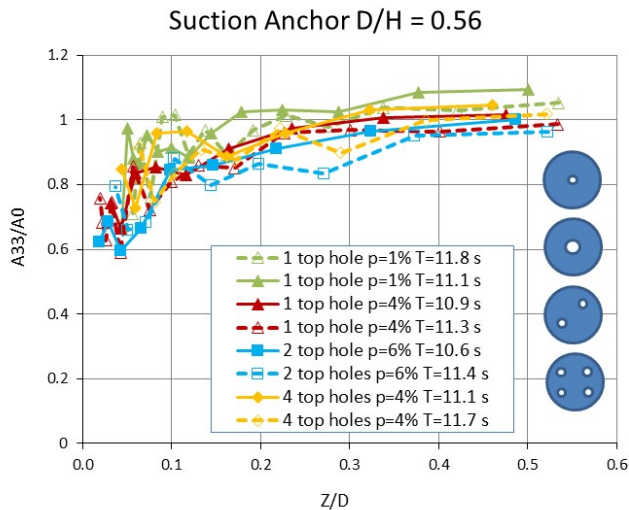


FIGURE 14. ADDED MASS FOR ANCHORS WITH ONE OR MORE CIRCULAR TOP HOLES. ANCHOR TYPE C.

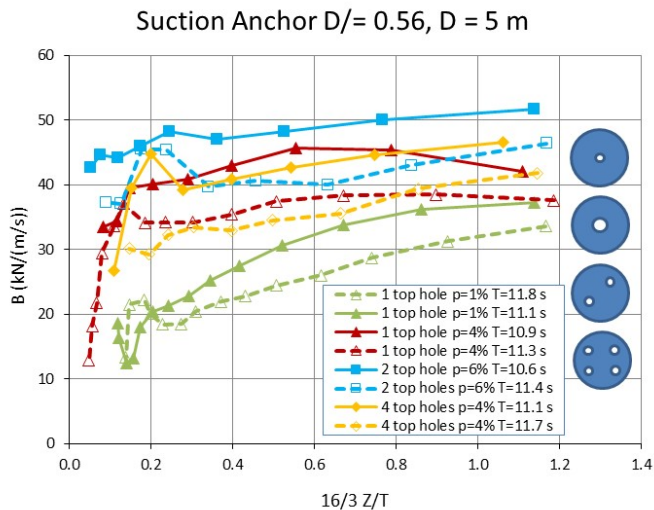


FIGURE 15. DAMPING FOR ANCHORS WITH ONE OR MORE CIRCULAR TOP HOLES. ANCHOR TYPE C.

**EFFECT OF VENTILATION**

B.Molin has in several publications, e.g. in Molin and Nielsen 2004 [4] showed that viscous flow through a porous disk influences both damping and added mass significantly. He introduced the porous KC number, a parameter that relates directly to the flow through the porosity and the pressure loss over the porous structure.

The porous KC number can be defined as:

$$KC_{por} = \frac{Z}{D} \cdot \frac{(1-p)}{2\mu \cdot p^2} \quad (4)$$

The added mass and the damping will vary with oscillation amplitude and will be dependent on KCpor. In [2] it was shown

that the curves of added mass for hatch covers with significantly different porosity gathered to express a common, well defined curve.

A similar exercise is performed for the suction anchors. For each anchor type and perforation a trend curve is drawn from the model test results, as illustrated in FIGURE 16 for anchor type D.

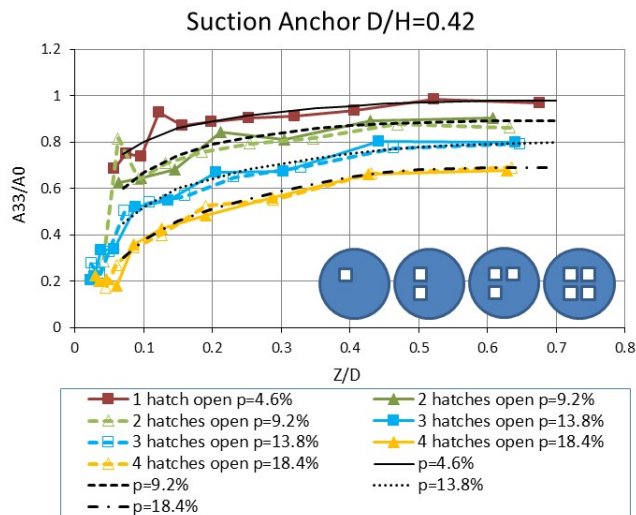


FIGURE 16. ADDED MASS FOR SUCTION ANCHORS WITH RECTANGULAR HOLES IN THE TOP PLATE. ANCHOR TYPE D. MODEL TEST RESULTS AND TREND LINES (BLACK) FOR EACH DEGREE OF PERFORATION.

Assembling the trend lines for anchor type A, C and D, with diameter/height relations of the same order of magnitude and plotting them as function of KCpor times the pressure loss parameter show that also for the anchors there is a connection between the different results, as shown in FIGURE 17.

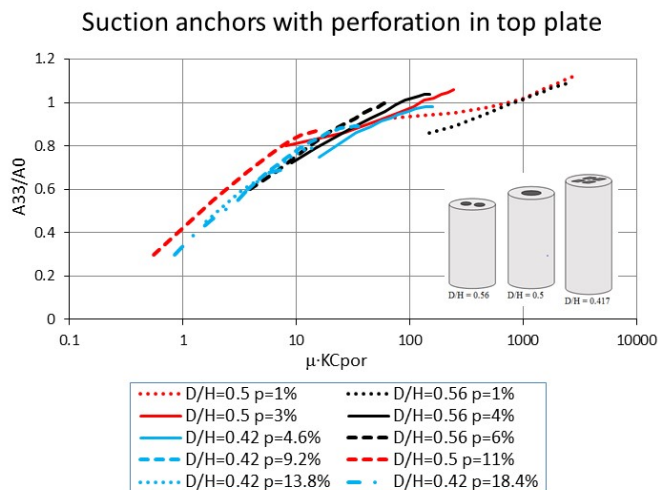
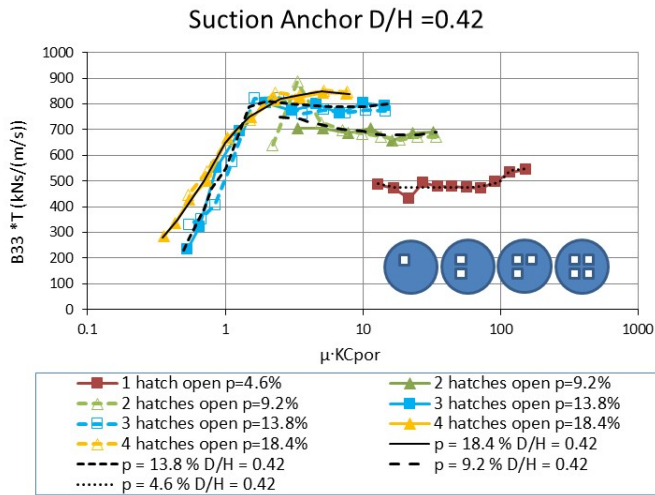
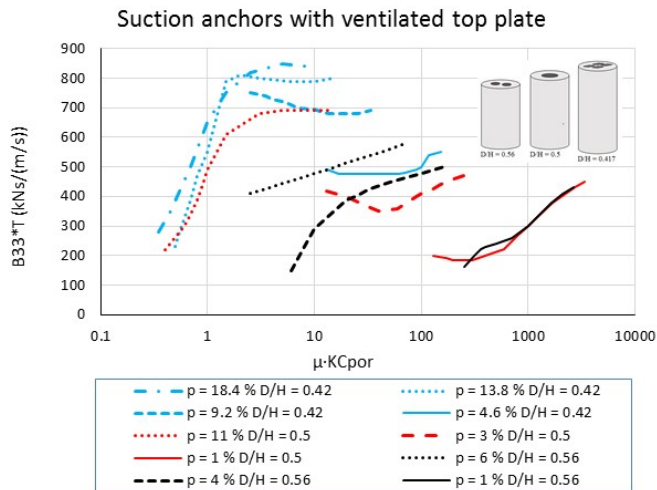


FIGURE 17. SUMMARY OF ADDED MASS FOR SUCTION ANCHORS WITH DIFFERENT PERFORATION OF THE TOP PLATE PLOTTED AS FUNCTION OF PORPUS KC NUMBER TIMES PRESSURE LOSS PARAMETER.

A similar exercise is performed for the damping, as shown in FIGURE 18 for anchor type D. Here damping times period of oscillation is plotted as function of porous KC number times pressure loss parameter. The trend lines for anchor type A, C and D are shown together FIGURE 19. The results for the two anchors with 1% perforation is similar. For the other perforations the results with perforation of similar order of magnitude are grouped together, but a clear trend in the results similar to the one for added mass is not observed. The same  $\mu \cdot KC_{por}$  number gives a  $B_{33}T$  value between 300 kNs/(m/s) and 800 kNs/(m/s) dependent on anchor type and perforation.



**FIGURE 18. DAMPING TIMES PERIOD OF OSCILLATION FOR SUCTION ANCHORS WITH RECTANGULAR HOLES IN THE TOP PLATE. ANCHOR TYPE D. MODEL TEST RESULTS AND TREND LINES (BLACK) FOR EACH DEGREE OF PERFORATION.**



**FIGURE 19. SUMMARY OF DAMPING TIMES PERIOD OF OSCILLATION FOR SUCTION ANCHORS WITH DIFFERENT PERFORATION OF THE TOP PLATE PLOTTED AS FUNCTION OF POROUS KC NUMBER TIMES PRESSURE LOSS PARAMETER.**

In FIGURE 20 damping times period of oscillation for different  $\mu \cdot KC_{por}$  values are plotted as function of perforation of the top plate. It is seen that the damping will increase for increasing perforation of the top plate.

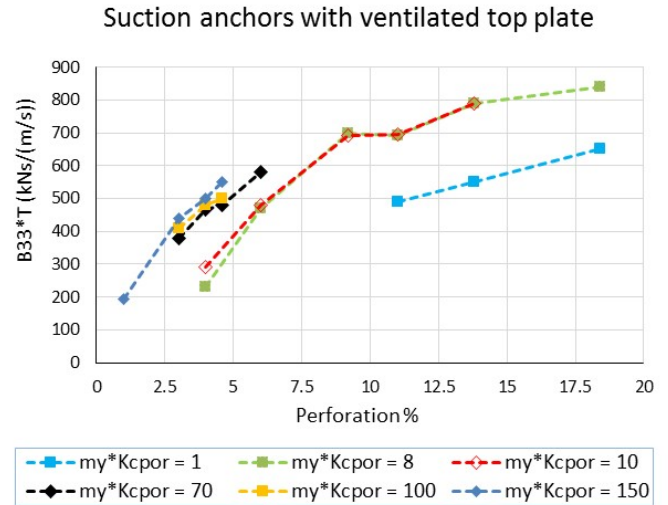


**FIGURE 20. DAMPING TIMES PERIOD OF OSCILLATION FOR DIFFERENT  $\mu KC_{por}$  VALUES AS FUNCTION OF PERFORATION OF THE TOP PLATE.**

The relation between damping and mass (expressed by  $B \cdot T / A$ ) is shown in FIGURE 21 for anchor type C with circular top hole(s). Similar to the results shown in FIGURE 11 it is seen that the importance of damping relative to added mass is getting larger when the perforation increases. The ratio appears to be little sensitive to the number of holes.

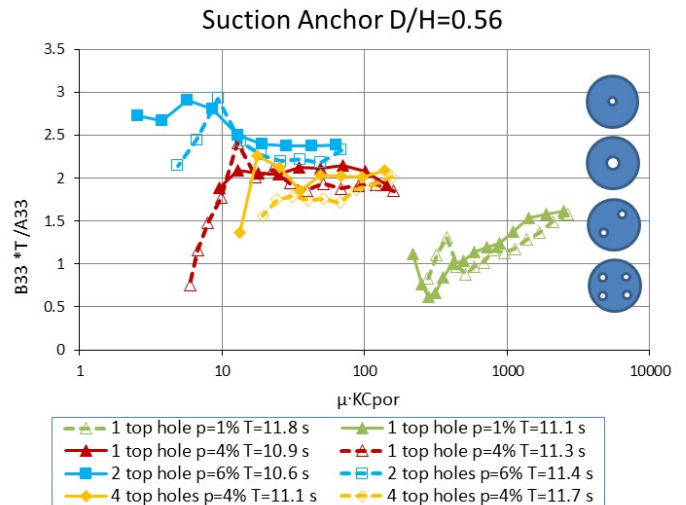


**FIGURE 21. DAMPING TIMES PERIOD OF OSCILLATION DIVIDED BY ADDED MASS AS FUNCTION OF  $\mu KC_{por}$  FOR ANCHORS WITH CIRCULAR TOP HOLE(S).**

A model test program to find hydrodynamic coefficient for a suction anchor with  $D/H = 1.0$  has been presented in Ireland et. al 2007 [5]. The top plate was ventilated by a set of circular holes placed close to the periphery. The motion decay method was used. The ventilation area was varied by opening or closing pairs of holes, giving ventilation area ratios of 0.8%, 1.6%, 2.4% and 4.8%. The motion decay was arranged from three defined initial offsets (0.3, 0.6 and 0.9 m full scale). These offsets are smaller than wave amplitudes but representative for crane amplitudes in operational sea states.

The tests indicated that the added mass and damping were amplitude dependent. However, average values of added mass and linear and quadratic damping derived from each motion decay were presented.

In FIGURE 22 the added mass as function of ventilation ratio in [5], denoted  $IMD_{xx}$ , is compared to the range of values for various suction anchors shown in FIGURE 17, denoted 'MT\_lo' and 'MT\_hi'. Tentative porous KC numbers are established, based on the perforation ratios and the reported range of decay amplitudes. FIGURE 22 show a good agreement.

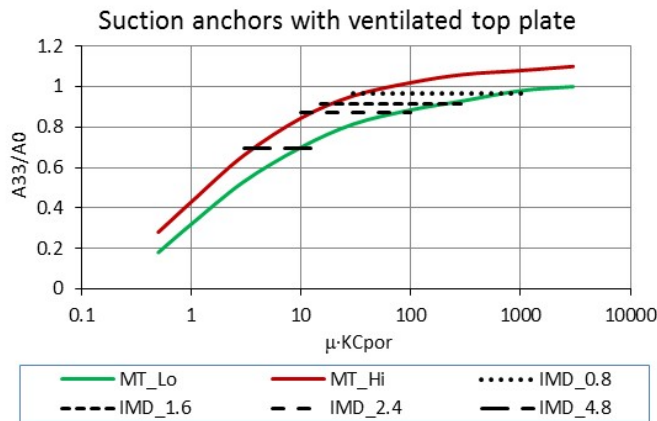


**FIGURE 22. ADDED MASS FOUND BY IRELAND ET. AL. [5], DENOTED "IMD\_xx" COMPARED TO THE RANGE OF VALUES PRESENTED IN FIGURE 17, DENOTED MT\_xx.**

## DISCUSSIONS AND CONCLUSION

For the diameter to height ratios studied, added mass for suction anchors without perforation has a small dependency of amplitude of oscillation. But, for practical purposes the added mass can be estimated to be equal to the displacement of a cylinder with the same diameter and height as the anchor plus the displacement of a circular sphere with the same diameter.

The damping is dependent on diameter to height ratio, amplitude and period of oscillation. Both linear and quadratic damping will be present.

For suction anchors with perforation of the top plate the added mass decreases and the damping increases for increasing degree of perforation. The added mass is close to the values for anchors without perforation when the perforation is less than 2 to 3 percent.

The presented added mass values show a good agreement with results published in Ireland et. al [5].

Damping is dependent on amplitude of oscillation and perforation. Increasing perforation will increase the linear contribution to the damping,  $B_1$ , and decrease the quadratic contribution,  $B_2$ . This is in accordance with the results from Ireland et. al [5]. A general trend of the damping results is that for perforations larger than around 10%, the damping is mainly quadratic for small amplitudes of oscillations and linear for larger amplitudes. For smaller perforations the damping contains both a linear and a quadratic term.

The derived data can be used in analysis considering harmonic design waves. However, the amplitude dependence of both added mass and damping is a challenge when coefficients are to be estimated and used in numerical tools for simulation of installation operations in irregular waves.

## ACKNOWLEDGMENTS

This work has been performed as a part of the research program MOVE, started in 2015 by NTNU, MARINTEK and SINTEF.

## REFERENCES

- [1] Recommended Practice "Modelling and Analysis of Marine Operations", DNVGL RP H-103, Feb. 2014
- [2] Sandvik, P.C, Solaas, F., Firoozkoobi, R.: "Hydrodynamic forces on complex subsea structures" MOSS2016, Singapore, Sept. 2016
- [3] Karlsen, L.G: "Modelling of hydrodynamic forces on underwater modules during installation" (in norwegian). MSc Thesis, NTH, Faculty for marine technology, Institute for marine hydrodynamics, Des. 1993.
- [4] Molin, B., Nielsen, F.G.: "Heave added mass and damping of a perforated disk below the free surface". 20th Intl. Workshop on Water waves and Floating bodies, Cortona, Italy, March, 2004.
- [5] Ireland, J, Macfarlane, G., Drobyshevski, Y.: "Investigation onto the sensitivity of the dynamic hook load during subsea deployment of a suction can". Proc. Of 26<sup>th</sup> Intl. Conf on Offshore Mechanics and Arctic Engineering, June 2007, San Diego, USA. Paper no. OMAE2007-29244.